THE JOURNAL OF PHYSICAL CHEMISTRY C

Article

Cite This: J. Phys. Chem. C 2019, 123, 29461−29467

pubs.acs.org/JPCC

CO_2 Viscosification by Functional Molecules from Mesoscale Simulations

Armando Gama Goicochea[†,‡] and Abbas Firoozabadi[*,†,§]

[†]Reservoir Engineering Research Institute, Palo Alto, California 94301, United States

[‡]Departamento de Ingeniería Química y Bioquímica, Tecnológico de Estudios Superiores de Ecatepec, Ecatepec de Morelos 55210, Estado de México, Mexico

[§]Department of Chemical and Biomolecular Engineering, Rice University, Houston, Texas 77005, United States

Supporting Information

ABSTRACT: The viscosity increase of carbon dioxide by copolymers is predicted using dissipative particle dynamics simulations, as a function of polymer concentration. Three types of direct viscosifying polymers are simulated: a fluorinated acrylate polymerized with styrene and two nonfluorinated copolymers. The latter are the hydrocarbon-based poly(1-decene), which is branched, and the linear poly(vinyl ethyl ether). These polymers associate differently in CO_2 because of their different molecular and chemical characteristics. The effect of different association mechanisms in increasing the viscosity of CO_2 is investigated in detail. It is found that intermolecular interactions and branched structure contribute to CO_2 thickening. In the fluorinated copolymer, intermolecular π-stacking interactions significantly affect CO_2 viscosification. These are the first simulations of the viscosity of CO_2 thickeners; our simulations agree with recent experimental data, providing insights into the thickening mechanisms at play of each molecule. This work sets the stage for the molecular engineering of new CO_2 viscosifiers.

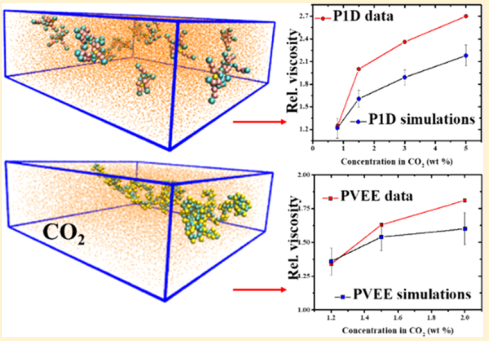

INTRODUCTION

There are important features that make carbon dioxide (CO_2) an attractive solvent, such as high diffusivity and relatively low cost, among others. However, some challenges limit wider use, including the low solubility of many large molecules, such as large alkanes in CO_2.[1,21,2] In enhanced oil recovery and as a clean fracturing fluid, CO_2 has desirable properties, but due to low viscosity, widespread use is limited. Under typical conditions found in oil reservoirs, CO_2 density is liquid-like, while its viscosity is gas-like.[3] The idea of thickening CO_2 with direct viscosifiers was pioneered by Heller et al. in 1985;[4] none of the polymers they examined thickened CO_2 by more than 10%. Heller et al.[4] found that polymers with high molecular weight showed low solubility to be useful as CO_2 thickeners, while polymers with low molecular weight led to minor viscosification. One may increase the viscosity of CO_2 substantially by adding high-molecular-weight fluorinated copolymers that are highly soluble in CO_2.[5,6] The relative increase in viscosity at a low shear rate can be over 200 times for a copolymer concentration of about 5 wt %, with respect to the viscosity of neat CO_2.[7] There are two serious shortcomings with this approach: the fluorinated copolymers are environmentally harmful and very expensive.[8] They are known to adsorb on rocks also, which reduces their efficiency.[9,10] It has been reported[11] that molecules with aromatic rings (such as polyfluoroacrylate-based copolymers) have higher adsorption on solid surfaces than molecules without the rings. Wang et al.[11] argue that the adsorption mechanism is driven by the "flatness" of the aromatic rings, which tends to reduce the free energy of the adsorbed molecules. To avoid these limitations, hydrocarbon-based copolymers without aromatic rings have been suggested as direct CO_2 viscosifiers.[12,13] The relative viscosity gain in CO_2 with these nontoxic copolymers is a factor less than 3 at a concentration of 5 wt %,[7] but their benign environmental characteristics and low cost make them attractive alternatives. The use of low-molecular-weight poly(1-decene) (P1D) and poly(vinyl ethyl ether) (PVEE) as CO_2 thickeners remains controversial because Zhang and co-workers reported CO_2 viscosification increases of about 15 times with P1D and PVEE at concentrations less than 1 wt % and a pressure of 20 MPa.[12] Heller et al.[4] and Lee et al.[14] also used P1D and PVEE in CO_2 at similar concentration and pressure, finding low to no increase in its viscosity. Al Hinai and co-workers[13] also measured the CO_2 viscosification effect of P1D and PVEE, at higher concentration (up to 5 wt %) and pressure (up to 55 MPa), finding viscosity increments up to 2.8 times for P1D (5 wt %, 55 MPa) and up to 2.1 times for PVEE (2 wt %, 55 MPa). For CO_2, we have not found reports in the literature on viscosification by relatively low molecular weight (M_w) polymers, such as P1D and PVEE.[12,13] However,

Received: September 9, 2019
Revised: November 6, 2019
Published: November 7, 2019

DOI: 10.1021/acs.jpcc.9b08589
J. Phys. Chem. C 2019, 123, 29461−29467

for aqueous solutions, the hydrophobically modified ethoxylated urethanes (HEUR) are low M_w, linear polymers that can thicken fluids at low concentrations.[15,16] Barmar et al.[15] have shown that HEUR polymers with a molecular weight of only 6410, comparable to PVEE's, can increase the viscosity of water at least 3 orders of magnitude at concentrations of around 4 wt % and less. The thickening mechanism has been attributed to the formation of networks, starting at the critical association concentration.[15] There are reports[17−19] where polymers with relatively low M_w are shown to notably thicken solvents at concentrations as low as 5 wt %.

In a recent work,[20] we investigated the structure of the hydrocarbon-based direct viscosifiers, poly(1-decene), or P1D, and poly(vinyl ethyl ether), PVEE, at low concentration in CO_2. Our investigation also covered a very effective fluorinated copolymer, polyheptadecafluorodecyl acrylate polymerized with styrene (HFDA).[7] It was concluded that the high solubility in CO_2 from fluorocarbon branches of HFDA and π-stacking interactions between styrene rings are key features in the intermolecular association. P1D disperses in CO_2 because it is a branched copolymer, which makes it soluble in CO_2 at concentrations similar to HFDA but at substantially higher pressure. Because P1D lacks aromatic rings, it does not form stable intermolecular associations. The linear PVEE copolymer forms weakly bound networks, and its solubility in CO_2 is lower than P1D.[4,13] Given the different association mechanisms displayed by these three molecules, the main objective of this work is to predict the viscosity of these functional molecules in CO_2 at low concentrations and develop a molecular understanding of their viscosification of CO_2. Comparing experimental reports, one finds that it is not only their associating mechanisms that make HFDA different from P1D and PVEE. It is also the fact that the HFDA polymer used in experiments[7] has M_w that can be 2 orders of magnitude higher than that of P1D and PVEE.[21] There is no report in the literature on CO_2 viscosification by molecular simulations, to the best of our knowledge. In this work, we report dissipative particle dynamics (DPD)[22−24] simulations of P1D, PVEE, and HFDA in CO_2 under stationary flow to calculate the shear viscosity as a function of concentration at high pressure. The simulations are compared with the experimental data. Figure 1 shows the coarse-grained structure of the three copolymers, with the atoms grouped into each DPD bead listed below each structure.[20] Figure 1a shows the P1D molecule, with a molecular weight of M_w = 910 g/mol. Each of its nine carbon branches is grouped into three DPD beads. In Figure 1b, one finds the structure of PVEE, with M_w = 3822 g/mol, as is found in experiments.[13] The structure of HFDA is displayed in Figure 1c; its molecular weight is M_w = 3970 g/mol, which compares with the value used by Sun et al.,[25] M_w = 3941 g/mol, for the same molecule. Huang and co-workers[7] do not report the molecular weight of the HFDA molecule used in their viscosity experiments; other groups that use the same molecule report molecular weights ranging from 146 000 to 540 000 g/mol.[2,21,26] Modeling molecules with such a large molecular weight at concentrations comparable with those of the experiments[7] is not practical because of the very long time required by the simulations with current computational resources. Yet, as we shall show here, much can be learned with the basic HFDA molecule shown in Figure 1c.

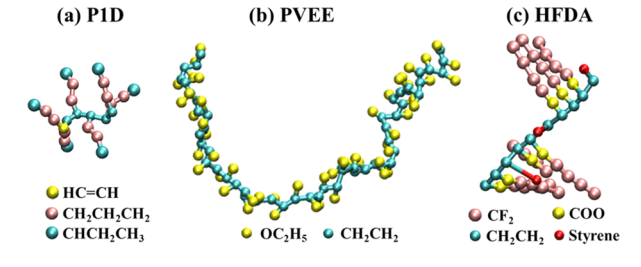

Figure 1. DPD models of the copolymers simulated in this work. (a) Poly-1-decene (P1D), $[CH_2CH[(CH_2)_7CH_3]]_n$, with n = 6, M_w = 910 g/mol. (b) Poly(vinyl ethyl ether) (PVEE), $[CH_2CH(OC_2H_5)]_n$, with n = 53, M_w = 3822 g/mol. (c) Polyheptadecafluorodecyl acrylate polymerized with styrene $C_{25}H_{40}O_2(C_8F_{17})_x(C_6H_5)_y$ (HFDA), with x = 7, y = 3, M_w = 3970 g/mol.

The DPD model is widely used,[27] and for brevity, only the pertinent information is presented with full details in the Supporting Information. The interaction data between the various DPD beads that make up the molecules are taken from our recent publication,[20] where they were obtained from their solubility parameter using the Groot−Warren methodology.[24] The temperature and pressure dependencies of solubility parameters were taken into account, and several tests were carried out to confirm the accuracy of our model.[20] The density of CO_2, the water−CO_2 interfacial tension, and the P1D−CO_2 and PVEE−CO_2 interfacial tensions were predicted using those DPD interactions, and an excellent agreement with experimental reports was achieved.[20]

RESULTS AND DISCUSSION

In the simulation of shear viscosity, we use the setup illustrated in Figure 2a, where two featureless parallel walls bound the fluid perpendicularly to the z-axis. The two fixed walls with separation distance D are modeled as short-ranged, linearly decaying forces acting along the z-axis given by the simple force law $F_w(z) = a_w[1 - z/z_C]$, for $z \le z_C = 0.4r_C$ and zero otherwise.[28] Here, a_w is the wall force amplitude, z_C is the maximum range of the wall force, and r_C is the DPD cutoff length.[28] The wall force amplitude a_w is chosen such that the simulated slope of the velocity profile coincides with the expected constant velocity gradient, $dv_x/dz = 2v_{x0}/D$. A constant velocity along the x-direction, v_{x0}, is applied only to those CO_2 beads closest to the wall, and a velocity equal in magnitude but opposite in direction is applied to the CO_2 beads closest to the opposite wall. This procedure minimizes the slip length and avoids artificial adsorption of the copolymers. The CO_2 beads that are within a distance $z \le 0.15r_C$ of each wall are assigned zero velocity along the z-direction, to avoid slip.[29−31] Such setup gives rise to a linear velocity gradient along the z-direction, once the stationary state is reached, as shown in Figure 2b. Periodic boundary conditions are applied in the x- and y-directions, but not along the z-axis, since the walls are placed perpendicularly to that direction. The velocity profile presented in Figure 2b, a typical example from our simulations, is characteristic of linear flow, known as the Couette flow.[32] The setup shown in Figure 2a with the effective wall forces alleviates the need to resort to higher density walls of frozen particles because the DPD beads do not penetrate the walls.[33,34]

Known artifacts introduced in the velocity profiles when using the Lees−Edwards (LE) periodic boundary conditions[35] are also avoided. Some of the issues that arise when using the LE method were partially circumvented[36] by setting to zero the dissipative and random DPD forces of the particles that cross the boundaries. However, those forces contribute crucially to

DOI: 10.1021/acs.jpcc.9b08589
J. Phys. Chem. C 2019, 123, 29461−29467

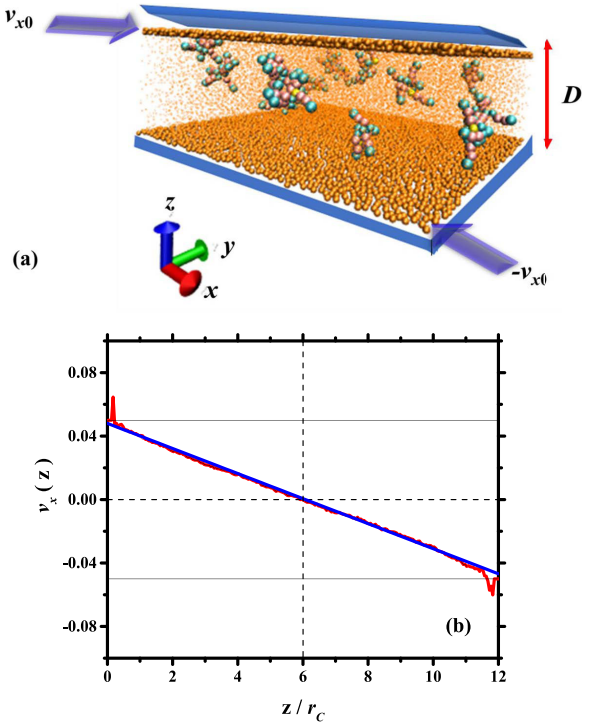

Figure 2. (a) Setup of stationary flow. Orange colored dots represent CO_2 beads under flow; yellow, pink, and cyan beads belong to P1D copolymers. The walls (in blue) perpendicular to the z-axis are separated by a constant distance, D, and are always at rest. A thin CO_2 layer is formed by the particles closest to the surfaces, shown as orange spheres. To avoid slippage, their z-component velocity is set to zero, $v_z(z = 0) = 0$, $v_z(z = D) = 0$. An additional constant velocity along the x-axis, $v_{x0} = 0.05 r_{C/\delta t}$, imparts a velocity gradient to the fluid bound by the surfaces, as indicated by the arrows. (b) Velocity profile (red line) from the simulations for a system of nine PVEE molecules in CO_2 (P = 53 MPa, T = 358 K, 44 046 CO_2 molecules). The best linear fit is shown as the blue line. The cutoff radius is r_C = 6.4 Å, and the time step is δt = 3 ps.

the viscosity,[35] and neglecting them yields underestimated values of the viscosity even at low shear rates. Alternative methods such as the Green−Kubo calculations of the viscosity tend to be noisy and are computationally demanding even for the DPD model.[30,37,38] The implicit walls used here have the additional advantage of having a controllable range, through the z_C parameter (vide supra), which helps reduce the slip length.[38] In particular, Figure S3 in the Supporting Information shows that even though the particle concentration profile displays structuring near the walls, as is always the case with molecules near surfaces, the velocity profile remains linear. The slip length is negligible, as is also the depletion layer[31] near the walls. One needs to keep the slip velocity and depletion layer small, since they tend to artificially reduce the viscosity;[31] the method we use achieves both. Additional details are provided in the Supporting Information.

The measurements of shear viscosity have been conducted using the falling cylinder viscometer[7] and the high-pressure−high-temperature capillary viscometer.[13] In the former, a small aluminum cylinder falls through the polymer-thickened CO_2 under fixed temperature and pressure and its terminal velocity (v_t) is measured; then, the viscosity of the fluid is obtained from the relation[7] $\eta = K(\rho_s - \rho_f)/v_t$. Here, K is the viscometer calibration constant, and ρ_s and ρ_f are the densities of the cylinder and the fluid, respectively. The capillary viscometer measures the pressure drop in a long capillary tube where the fluid flows at a known constant rate, and the viscosity is determined from the Hagen−Poiseuille equation.[13] Both methods can be modeled as stationary flow.

In this work, the viscosity, η, is obtained from the stress tensor along the x-direction, P_x, averaged over the entire width, D, divided by the shear rate $\dot{\gamma}$[32]

$$\eta = \frac{\langle P_x \rangle}{\langle \dot{\gamma} \rangle} \tag{1}$$

The x-component of the stress tensor in eq 1 is calculated from $\langle P_x \rangle = \langle F_x \rangle / A$, where F_x is the force acting on the beads along the x-direction averaged over all of the particles and over time, and A is the transversal area of the walls. The shear rate is given by the gradient of the x-component of the velocity of the fluid along the z-direction, $\dot{\gamma} = \nabla v_x$. If the flow is linear, the gradient is constant, and for the setup illustrated in Figure 2a, $\dot{\gamma} = 2v_{x0}/D$. Equation 1 is ideally suited for the calculation of the viscosity by molecular simulations because both quantities that define it, the shear stress and the shear rate, are obtained directly from the simulations as molecular averages. We first calculate the viscosity of pure CO_2 at two thermodynamic conditions (20 MPa/329 K and 53 MPa/377 K) and compare it with the experimental data. The viscosity of pure P1D liquid is also predicted and compared with the data. The results, presented in Table 1, show an agreement with experiments and verify the simulation setup presented in Figure 2 for the calculation of the shear viscosity.

Table 1. Viscosity of CO_2 and P1D

fluid	T (K)	P (MPa)	measured viscosity (cP)	predicted viscosity (cP)
CO_2	329	20	0.063[12]	0.059 ± 0.005
CO_2	377	53	0.076[13]	0.075 ± 0.004
P1D	313	0.1	42.0[39]	42.3 ± 0.5

To further examine the robustness of the method to simulate the shear viscosity, we carried out simulations of PVEE in CO_2 under various cell sizes, testing for finite size effects. PVEE is the largest molecule modeled in this work, and it may be more susceptible to finite size effects than P1D or HFDA. The results are presented in Table 2.

Table 2. Finite Size Effect in the Viscosity of CO_2 with PVEE at 1.5 wt %, 53 MPa/358 K

cell dimensions (nm^3)	simulation time (ns)	predicted viscosity (cP)
20.1 × 20.1 × 3.9	500	0.099 ± 0.003
32.8 × 32.8 × 3.9	200	0.092 ± 0.002
23.2 × 23.2 × 7.8	100	0.096 ± 0.003
16.4 × 16.4 × 15.6	100	0.093 ± 0.005

The last column in Table 2 lists our predictions for the viscosity of the fluid mixture of CO_2 with 1.5 wt % PVEE as a function of the cell's size; there is an agreement with the experimental value $\eta = 0.104 \pm 0.001$ cP.[13] The results indicate no appreciable finite size effect. This conclusion confirms previous reports for both equilibrium[40] and shear viscosity calculations[41] and is a consequence of the short-ranged nature of the DPD forces[23,24] and the stability of the thermostat.[42]

Figure 3 shows the snapshots from our simulations under the Couette flow. Figure 3a,b corresponds to the hydrocarbon-

DOI: 10.1021/acs.jpcc.9b08589
J. Phys. Chem. C 2019, 123, 29461−29467

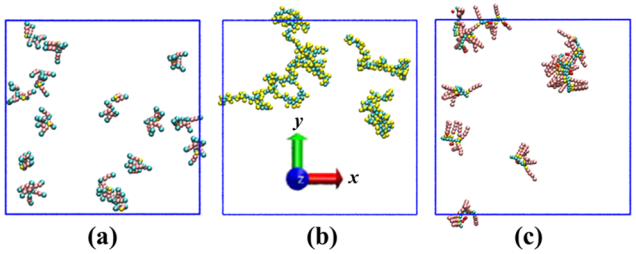

Figure 3. Typical snapshots of the *xy*-plane of the structure of copolymers in CO_2 under shear flow. (a) Fifteen P1D molecules in 44 640 CO_2 beads at 53 MPa/358 K and concentration 0.8 wt %; the volume of the simulation box is 23 × 23 × 8 nm^3. (b) Five PVEE molecules and 44 470 CO_2 beads, also at 53 MPa/358 K and concentration 1.2 wt %. The simulation box volume is 23 × 23 × 8 nm^3. (c) Twelve molecules of HFDA in 51 924 CO_2 beads at 34 MPa/298 K and at a concentration of 2.0 wt % in a box of dimensions 27.1 × 27.1 × 6.5 nm^3. The shear is applied along the *x*-axis. The CO_2 beads are omitted for clarity.

based copolymers P1D and PVEE, respectively, while Figure 3c shows the structure of the fluorinated copolymer HFDA. P1D displays a markedly different behavior from PVEE: while the latter forms entangled networks, the former disperses in the fluid, forming no molecular associations. The P1D molecule[13] has six branches; see Figure 1a. Figure 3a reveals that the branches extend into the CO_2 medium. The radial distribution functions of those branches at the atomistic and mesoscopic scales show[20] that the "spreading" formation of those branches is a consequence of the solubility of P1D in CO_2. The number of CO_2 molecules surrounding PVEE is found to be lower than in P1D,[20] which is consistent with the experimental data that the solubility of PVEE is lower than that of P1D in CO_2 at the same conditions.[13] Figure 3b shows that PVEE forms entangled associations with other molecules of its kind, although they tend to form and break up intermittently. The behavior of the fluorinated HFDA, in Figure 3c, is more complex. Its branches are composed of fluorocarbon beads, which are known to be highly soluble in CO_2.[2] The highest CO_2 viscosification is obtained when the HFDA molecule contains 30% of styrene and 70% of fluorocarbon units.[7] We have selected this composition for the molecule in our simulations. The styrene beads, shown in red in Figure 3c, are the key ingredient that keeps the HFDA agglomerates stable over time, through π-stacking interactions.[26] We have found[20] that in the HFDA composition we have modeled, the intermolecular π-stacking interaction is predominant over the intramolecular π-stackings, leading to aggregation. These contrasting structuring mechanisms under flow are in agreement with the results from equilibrium DPD simulations[20] and reveal the origin of the viscosification differences, as seen in Figure 4.

The comparison between the simulated viscosity vs concentration for the nonfluorinated P1D and PVEE, and the data,[13] is shown in Figure 4a. The comparison with data[7] for HFDA is shown in Figure 4b. Our simulations are in agreement with the experimental data and follow the same trends. These simulations show contrasting behavior between the fluorinated and nonfluorinated copolymers; HFDA increases the CO_2 viscosity at least 2 orders of magnitude more than P1D and PVEE. The trends are also very different: while the viscosity increase with copolymer concentration is approximately linear for P1D and PVEE, in Figure 4a, it is

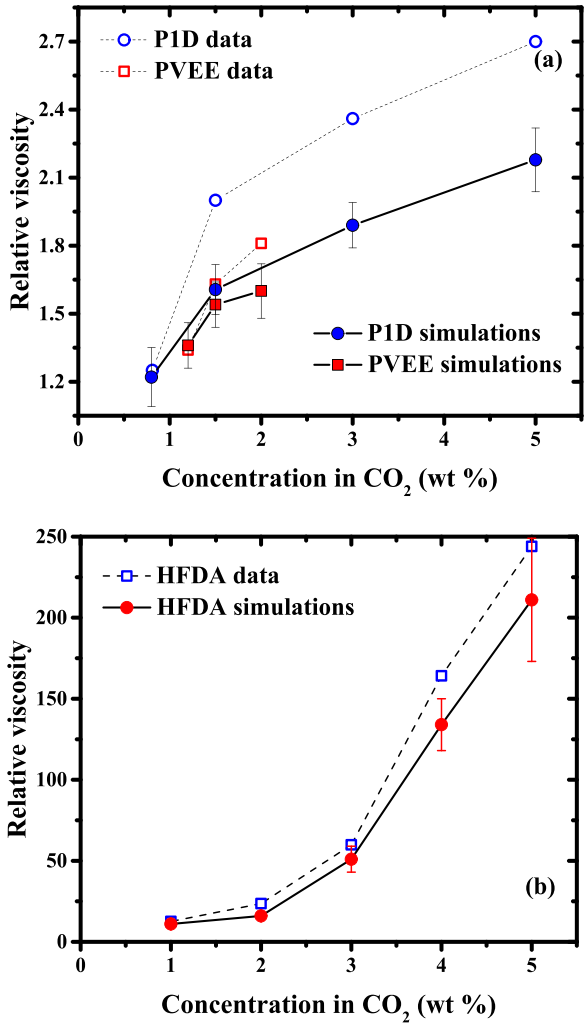

Figure 4. Comparison of the simulated relative viscosity of CO_2 with direct thickeners and measured data for (a) nonfluorous copolymers (at P = 53 MPa, T = 358 K) and (b) fluorocarbon-based HFDA (at P = 34 MPa, T = 298 K). Experimental data are from (a) Al Hinai et al.[13] and (b) Huang et al.[7]

exponential for HFDA; see Figure 4b. If the solubility is plotted as a function of copolymer concentration, the same behavior is found, namely, linearly growing for P1D/PVEE, exponential like for HFDA.[20] Figures 3 and 4 reveal the reason P1D is a more effective thickener than PVEE because the branched structure increases the solubility, which, in turn, helps disperse P1D in CO_2. The uniform dispersion leads P1D molecules to change momentum from collisions under flow, which increases the viscosity; see eq 1. The fluorinated HFDA yields high viscosification because of two key aspects inherent to that molecule: its high solubility in CO_2 and intermolecular aggregation driven by π-stacking interactions. The latter forms locally dense structures whose momentum change under flow is large, while the former leads to the uniform dispersion of the aggregates in CO_2. These aggregates increase the intermolecular interactions among the polymers, which is a mechanism that has been used successfully in the design of aqueous viscosifiers[43] for some time. The process is based on the permanence over time of the aggregates. This is more clearly seen when comparing with the associations of PVEE chains, where networks are also formed and then broken, yielding relatively modest viscosity gains.

DOI: 10.1021/acs.jpcc.9b08589
J. Phys. Chem. C 2019, 123, 29461−29467

P1D has relatively high solubility in CO_2 due to its branched structure, but lacks an intermolecular coupling mechanism; therefore, the viscosity enhancement arises only from its volume fraction (ϕ) in the fluid. P1D molecules act as soft spheres dispersed in the medium; see Figure 3a. That explains why the dependence of P1D relative viscosity (η_{rel}) on concentration follows a linear trend, as expected from Einstein's model,[32] $\eta_{rel} = (1 + 2.5\phi)$. A high polymer concentration would be required to achieve a relative viscosity increase of about an order of magnitude. The operative thickening mechanism in PVEE is given by the formation of networks of polymer chains, which create resistance to flow (viscosity) at low shear, while the networks persist. However, these associations are broken by collisions between the monomers and the fluid, yielding low viscosity when averaged over time. To increase the viscosity of CO_2 with PVEE, high concentrations are required, as in P1D. PVEE is a relatively large molecule, which limits its solubility in the fluid,[44] as seen by the lower concentrations in Figure 4a. A synergistic effect in the viscosity is not expected if one adds a mixture of P1D/PVEE to CO_2 because the intermolecular interactions between their monomers are very weak to yield stable networks. The thickening characteristics of HFDA for CO_2 stem from two aspects: high solubility in CO_2, due to its branched structure and to the fluorocarbon units along its branches (see Figure 1c), and its intermolecular coupling mechanism. The latter is provided by the styrene rings, which yield intermolecular, π-stacking associations that are stable over time[14] and under flow; see Figure 3c. The diffusion of these aggregates in the solvent is reduced because they become heavier; hence, the viscosity increases. It has been shown[20] that for the specific HFDA composition used in this work, and shown in experiments[7] to be the most effective, intermolecular π-stacking interactions dominate over intramolecular π-stackings. This makes the HFDA aggregates very stable over time, thickening CO_2 through a mechanism similar to the one that is operative in aqueous associative thickeners,[45] i.e., forming associations of aggregates. The viscosity of these aggregates no longer follows a linearly increasing function of polymer concentration, but it is represented by a power law function,[46] as seen in Figure 4b. Since the true molecular weight of the HFDA copolymer used in experiments may be some 2 orders of magnitude higher[21] than the one modeled here, the results for HFDA shown in Figure 4b indicate that the associative mechanism is mainly responsible for the thickening power. This helps explain why experiments with HFDA polymers without styrene rings,[7] responsible for the intermolecular association, give much lower thickening than those with them. Huang and co-workers[7] measured the relative viscosity gains of about 25 times only when HFDA does not contain styrene, at a polymer concentration of 8 wt %. Hence, the molecular weight appears to be of secondary importance, as it has been found to be the case for some aqueous thickeners.[15]

Despite the lower thickening capability of the nonfluorinated P1D when compared with that of HFDA, this polymer is a promising candidate that can serve as a template in the search for more efficient thickeners due to its solubility in CO_2. This is to be contrasted with large linear hydrocarbons that are essentially insoluble in CO_2 under conditions of interest.[44] As for HFDA, not only does it have environmental and economic issues but it may also adsorb onto rocks,[9,10] making it an untenable candidate for viscosification for improved oil recovery.

CONCLUDING REMARKS

We report the first work on molecular dynamics simulations, to the best of our knowledge, of the viscosity enhancement in CO_2 by three types of direct viscosifying copolymers. One effective copolymer (HFDA) has branches of fluorinated carbon units with styrene rings along its backbone. The other two are hydrocarbon-based copolymers, one having branches (P1D) and the other is linear (PVEE). The viscosifying mechanisms for the three have remained unclear. In this work, we investigate in detail their behavior in CO_2 under flow by nonequilibrium, stationary flow DPD simulations. Our results show that three different viscosifying mechanisms emerge in these copolymers. The branched hydrocarbon molecules disperse singly in CO_2, forming soft sphere-like units that increase the viscosity linearly. Increasing the volume fraction of this branched molecule leads to a linear increase in the viscosity of CO_2, as predicted by Einstein's model. The linear molecule is a relatively long polymer whose solubility in CO_2 is lower than that of the molecule with branches. Its thickening mechanism consists of the formation of entanglements between the copolymer molecules, which form networks that resist flow, thereby increasing the viscosity. Those networks are short-lived because their intermolecular entanglements are weak. The fluorinated molecule produces a much higher viscosity in CO_2 than the hydrocarbon-based copolymers. Our simulations show that its viscosification mechanism is a synergistic combination of two factors. The fluorocarbon units along its branches are highly soluble in CO_2, yielding extended branches into the fluid. The styrene rings create intermolecular π-stacking couplings that are strong enough to produce agglomerates that are stable under flow, leading to a substantial viscosity increase. The viscosity increase is not linear, as it is for the hydrocarbon copolymers, but it resembles a power law function with increasing concentration. This viscosifying mechanism is similar to that found in rheology modifiers of aqueous solutions, where molecules are tailored to form associations of agglomerates.

In the simulations of the viscosity, we have introduced an optimized calculation method. The stationary Couette flow is produced by bounding the fluid with implicit, linearly decreasing and short-ranged walls. These walls have two controllable parameters that help reduce artifacts typically found in simulations of the shear viscosity. One of those is the maximum range (z_C) of the wall force, which reduces the structuring of the fluid near the surface, as well as the slip length and the depletion layer. Those are factors that tend to artificially reduce the predicted value of the viscosity. The second controllable parameter of our wall model is its maximum amplitude (a_w), which is adjusted after extensive tests of the predicted velocity profile of the pure CO_2 fluid. The value of a_w is chosen to provide a linear velocity profile, which, in turn, predicts the correct shear viscosity of CO_2. The one-molecule thick layer of CO_2 molecules closest to the wall is imparted with a fixed velocity along the direction of flow (opposite to that of the other wall), and a linear velocity profile is obtained. The method is computationally inexpensive, and the viscosity predicted is in agreement with the data from the literature. Our work sets the stage to engineer new CO_2 viscosifiers. HFDA is known to be harmful to the environment, and very expensive and alternative CO_2 thickening molecules will be in high demand.

DOI: 10.1021/acs.jpcc.9b08589
J. Phys. Chem. C 2019, 123, 29461−29467

METHODS

DPD simulations are performed in the NVT ensemble. One CO_2 molecule is coarse-grained in one DPD bead. To form polymers, DPD beads are joined by freely rotating harmonic springs whose parameters k_0 and r_0 have been successfully tested before.[22] The simulations are performed in reduced units so that temperature, mass, and cutoff radius are $T = m = r_c = 1$, respectively. The time step used is $\delta t = 0.03$, and the global numerical density is always kept equal to 3 to ensure that the DPD equation of state remains invariant with respect to changes of interaction parameters. To dimensionalize energy, viscosity, length, and time, we use the thermal energy at room temperature, k_BT, r_c = 6.48 Å, δt = 3 ps, as is appropriate for a coarse-graining degree equal to three water molecules per DPD bead. The simulations are run for at least 100 ns and up to 0.5 μs, with the first half used for reaching the steady state and the rest for the production phase.

ASSOCIATED CONTENT

Supporting Information

The Supporting Information is available free of charge on the ACS Publications website at DOI: 10.1021/acs.jpcc.9b08589.

DPD model and simulation details; DPD conservative force parameters and force interaction parameters; viscosity calculation details; spatial dependence of the short-ranged, linearly decaying surface force; schematic representation of the viscosity calculation setup (PDF)

AUTHOR INFORMATION

Corresponding Author

*E-mail: Abbas.Firoozabadi@rice.edu, af@rerinst.org.

ORCID

Abbas Firoozabadi: 0000-0001-6102-9534

Notes

The authors declare no competing financial interest.

ACKNOWLEDGMENTS

The authors would like to thank the member companies of the RERI for their support. A.G.G. would like to thank CONACYT for a sabbatical scholarship.

REFERENCES

(1) Peach, J.; Eastoe, J. Supercritical Carbon Dioxide: a Solvent Like no Other. *Beilstein J. Org. Chem.* **2014**, *10*, 1878−1895.

(2) DeSimone, J. M.; Guan, Z.; Elsbernd, C. S. Synthesis of Fluoropolymers in Supercritical Carbon Dioxide. *Science* **1992**, *257*, 945−947.

(3) Bachu, S. Sequestration of CO_2 in Geological Media in Response to Climate Change: Road Map for Site Selection Using the Transform of the Geological Space into the CO_2 Phase Space. *Energy Convers. Manage.* **2002**, *43*, 87−102.

(4) Heller, J. P.; Dandge, D. K.; Card, R. J.; Donaruma, L. G. Direct Thickeners for Mobility Control of CO_2 floods. *Soc. Pet. Eng. J.* **1985**, *25*, 679−686.

(5) Hoefling, T. A.; Stofesky, D.; Reid, M.; Beckman, E. J.; Enick, R. M. The Incorporation of a Fluorinated Ether Functionality into a Polymer or Surfactant to Enhance CO_2-Solubility. *J. Supercrit. Fluids* **1992**, *5*, 237−241.

(6) Cummings, S.; Xing, D.; Enick, R.; Rogers, S.; Heenan, R.; Grillo, I.; Eastoe, J. Design Principles for Supercritical CO_2 Viscosifiers. *Soft Matter* **2012**, *8*, 7044−7055.

(7) Huang, Z.; Shi, C.; Xu, J.; Kilic, S.; Enick, R. M.; Beckman, E. J. Enhancement of the Viscosity of Carbon Dioxide Using Styrene/Fluoroacrylate Copolymers. *Macromolecules* **2000**, *33*, 5437−5442.

(8) Kilic, S.; Enick, R. M.; Beckman, E. J. Fluoroacrylate-Aromatic Acrylate Copolymers for Viscosity Enhancement of Carbon Dioxide. *J. Supercrit. Fluids* **2019**, *146*, 38−46.

(9) Zaberi, H. A.; Lee, J. J.; Cummings, S. D.; Beckman, E. J.; Enick, R. M.; Dailey, C.; Vasilache, M. *Fluoroacrylate Polymers as CO_2-Soluble Conformance Control Agents. SPE-190176-MS*; Society of Petroleum Engineers, 2019.

(10) Li, Y.; Wang, Y.; Guo, G.; Wang, K.; Gomado, F.; Zhang, C. The Effect of Fluorocarbon Surfactant on the Gas Wetting Alteration of Reservoir. *Pet. Sci. Technol.* **2018**, *36*, 951−958.

(11) Wang, X.; Hu, Y.; Min, J.; Li, S.; Deng, X.; Yuan, S.; Zuo, X. Adsorption Characteristics of Phenolic Compounds on Graphene Oxide and Reduced Graphene Oxide: A Batch Experiment Combined Theory Calculation. *Appl. Sci.* **2018**, *8*, No. 1950.

(12) Zhang, S.; She, Y.; Gu, Y. Evaluation of Polymers as Direct Thickeners for CO_2 Enhanced Oil Recovery. *J. Chem. Eng. Data* **2011**, *56*, 1069−1079.

(13) Al Hinai, N. M.; Saeedi, A.; Wood, C. D.; Myers, M.; Valdez, R.; Sooud, A. K.; Sari, A. Experimental Evaluations of Polymeric Solubility and Thickeners for Supercritical CO_2 at High Temperatures for Enhanced Oil Recovery. *Energy Fuels* **2018**, *32*, 1600−1611.

(14) Lee, J. J.; Cummings, S.; Dhuwe, A.; Enick, R. M.; Beckman, E. J.; Perry, R.; Doherty, M.; O'Brien, M. *Development of Small Molecule CO_2 Thickeners for EOR and Fracturing. SPE−169039- MS*; Society of Petroleum Engineers, 2014.

(15) Barmar, M.; Ribitsch, V.; Kaffashi, B.; Barikani, M.; Sarreshtehdari, Z.; Pfragner, J. Influence of Prepolymers Molecular Weight on the Viscoelastic Properties of Aqueous HEUR Solutions. *Colloid Polym. Sci.* **2004**, *282*, 454−460.

(16) Suzuki, S.; Uneyama, T.; Inoue, T.; Hiroshi Watanabe, H. Nonlinear Rheology of Telechelic Associative Polymer Networks: Shear Thickening and Thinning Behavior of Hydrophobically Modified Ethoxylated Urethane (HEUR) in Aqueous Solution. *Macromolecules* **2012**, *45*, 888−898.

(17) Liu, K.; Kiran, E. Miscibility, viscosity and density of poly (ε-caprolactone) in acetone + CO_2 binary fluid mixtures. *J. Supercrit. Fluids* **2006**, *39*, 192−200.

(18) Pensado, A. S.; Pádua, A. A. H.; Comuñas, M. J. P.; Fernández, J. Viscosity and Density Measurements for Carbon Dioxide + Pentaerythritol Ester Lubricant Mixtures at Low Lubricant Concentration. *J. Supercrit. Fluids* **2008**, *44*, 172−185.

(19) Cook, R. L.; King, H. E., Jr.; Peiffer, D. G. High-Pressure Viscosity of Dilute Polymer Solutions in Good Solvents. *Macromolecules* **1992**, *25*, 2928−2934.

(20) Gama Goicochea, A.; Firoozabadi, A. Atomistic and Mesoscopic Simulations of the Structure of CO_2 with Fluorinated and Nonfluorinated Copolymers. *J. Phys. Chem. C* **2019**, *123*, 17010−17018.

(21) Xu, J.; Wlaschin, A.; Enick, R. M. Thickening Carbon Dioxide with the Fluoroacrylate−Styrene Copolymer. *SPE J.* **2003**, *8*, 85−91.

(22) Hoogerbrugge, P. J.; Koelman, J. M. V. A. Simulating Microscopic Hydrodynamic Phenomena with Dissipative Particle Dynamics. *Europhys. Lett.* **1992**, *19*, 155−160.

(23) Español, P.; Warren, P. B. Statistical Mechanics of Dissipative Particle Dynamics. *Europhys. Lett.* **1995**, *30*, 191−196.

(24) Groot, R. D.; Warren, P. B. Dissipative Particle Dynamics: Bridging the Gap Between Atomistic and Mesoscopic Simulation. *J. Chem. Phys.* **1997**, *107*, 4423−4435.

(25) Sun, W.; Sun, B.; Li, Y.; Fan, H.; Gao, Y.; Sun, H.; Li, G. Microcosmic understanding on thickening capability of copolymers in supercritical carbon dioxide: the key role of $\pi-\pi$ stacking. *RSC Adv.* **2017**, *7*, 34567−34573.

(26) Sun, W.; Sun, B.; Li, Y.; Huang, X.; Fan, H.; Zhao, X.; Sun, H.; Sun, W. Thickening Supercritical CO_2 with π-Stacked Co-Polymers: Molecular Insights into the Role of Intermolecular Interaction. *Polymers* **2018**, *10*, No. 268.

DOI: 10.1021/acs.jpcc.9b08589
J. Phys. Chem. C 2019, 123, 29461−29467

(27) Español, P.; Warren, P. Perspective: Dissipative Particle Dynamics. *J. Chem. Phys.* **2017**, *146*, No. 150901.
(28) Gama Goicochea, A. Adsorption and Disjoining Pressure Isotherms of Confined Polymers Using Dissipative Particle Dynamics. *Langmuir* **2007**, *23*, 11656−11663.
(29) Pivkin, I. V.; Karniadakis, G. E. A New Method to Impose No-Slip Boundary Conditions in Dissipative Particle Dynamics. *J. Comput. Phys.* **2005**, *207*, 114−128.
(30) Pastorino, C.; Binder, K.; Kreer, T.; Müller, M. Static and Dynamic Properties of the Interface Between a Polymer Brush and a Melt of Identical Chains. *J. Chem. Phys.* **2006**, *124*, No. 064902.
(31) Palmer, T. L.; Espås, T. A.; Skartlien, R. Effects of Polymer Adsorption on the Effective Viscosity in Microchannel Flows: Phenomenological Slip Layer Model from Molecular Simulations. *J. Dispersion Sci. Technol.* **2019**, *40*, 264−275.
(32) Batchelor, G. K. *An Introduction to Fluid Dynamics*; Cambridge University Press: New York, 2000.
(33) Xu, S.; Wang, Q. J.; Wang, J. A New Wall Model for Slip Boundary Conditions in Dissipative Particle Dynamics. *Int. J. Numer. Methods Fluids* **2019**, *90*, 442−455.
(34) Revenga, M.; Zúñiga, I.; Español, P. Boundary Conditions in Dissipative Particle Dynamics. *Comput. Phys. Commun.* **1999**, *121*−*122*, 309−311.
(35) Boromand, A.; Jamali, S.; Maia, J. M. Viscosity Measurement Techniques in Dissipative Particle Dynamics. *Comput. Phys. Commun.* **2015**, *196*, 149−160.
(36) Chatterjee, A. Modification to Lees−Edwards Periodic Boundary Condition for Dissipative Particle Dynamics Simulation with High Dissipation Rates. *Mol. Simul.* **2007**, *33*, 1233−1236.
(37) Keaveny, E. E.; Pivkin, I. V.; Maxey, M.; Karniadakis, G. E. A Comparative Study Between Dissipative Particle Dynamics and Molecular Dynamics for Simple- and Complex-Geometry Flows. *J. Chem. Phys.* **2005**, *123*, No. 104107.
(38) Xu, J.; Yang, C.; Sheng, Y.-J.; Tsao, H.-K. Apparent Hydrodynamic Slip Induced by Density Inhomogeneities at Fluid − Solid Interfaces. *Soft Matter* **2015**, *11*, 6916−6920.
(39) See www.sigmaaldrich.com.
(40) Velázquez, M. E.; Gama Goicochea, A.; González-Melchor, M.; Neria, M.; Alejandre, J. Finite-Size Effects in Dissipative Particle Dynamics Simulations. *J. Chem. Phys.* **2006**, *124*, No. 084104.
(41) Gama Goicochea, A.; Mayoral, E.; Klapp, J.; Pastorino, C. Nanotribology of Biopolymer Brushes in Aqueous Solution Using Dissipative Particle Dynamics Simulations: an Application to PEG Covered Liposomes in a Theta Solvent. *Soft Matter* **2014**, *10*, 166−174.
(42) Pastorino, C.; Kreer, T.; Müller, M.; Binder, K. Comparison of Dissipative Particle Dynamics and Langevin Thermostats for Out-Of-Equilibrium Simulations of Polymeric Systems. *Phys. Rev. E* **2007**, *76*, No. 026706.
(43) Tan, H.; Tam, K. C.; Jenkins, R. D. Network Structure of a Model HASE Polymer in Semi Dilute Salt Solutions. *J. Appl. Polym. Sci.* **2001**, *79*, 1486−1496.
(44) Rindfleisch, F.; DiNoia, T. P.; McHugh, M. A. Solubility of Polymers and Copolymers in Supercritical CO_2. *J. Phys. Chem. A* **1996**, *100*, 15581−15587.
(45) Maestro, A.; González, C.; Gutiérrez, J. M. Thickening Mechanism of Associative Polymers. *Macromol. Symp.* **2002**, *187*, 919−927.
(46) Bullard, J. W.; Pauli, A. T.; Garboczi, E. J.; Martys, N. S. A Comparison of Viscosity−Concentration Relationships for Emulsions. *J. Colloid Interface Sci.* **2009**, *330*, 186−193.

DOI: 10.1021/acs.jpcc.9b08589
J. Phys. Chem. C 2019, 123, 29461−29467